Performance of Multiple-Feed Metasurface Antennas with Different Numbers of Patch Cells and Different Substrate Thicknesses

Niamat Hussain and Ikmo Park

Department of Electrical and Computer Engineering
Ajou University, Suwon 16499, Republic of Korea
ipark@ajou.ac.kr

Abstract ─ The design and performance of low-profile, multiple-feed metasurface antennas with different numbers of patch cells and different substrate thicknesses at a terahertz frequency are presented in this paper. The utilized antenna designs consist of a periodic array $(N \times M)$ metallic square-patch metasurface and a planar feeding structure, which are both patterned on an electrically thin, high-permittivity GaAs substrate. The antenna gain increased in a linear fashion with an increasing number of patch cells, which were directly fed by the slit feedline. A 3-dB gain increment was observed irrespective of the substrate thickness when the number of patch cells was doubled. However, the 3-dB gain bandwidth as well as the radiation efficiency changed significantly with varying substrate thicknesses. The described antenna structure offers useful characteristics by means of a combination of different substrate thicknesses and patch numbers. In addition, the proposed antenna design features a number of benefits, including a low profile, mechanical robustness, easy integration into circuit boards, and excellent suitability for low-cost mass production.

Index Terms ─ Antenna array, metamaterials, metasurface, terahertz antennas, wide gain bandwidth.

I. INTRODUCTION

In recent years, metasurfaces have facilitated new approaches for manipulating the wavefronts of electromagnetic waves [1]. A metasurface is a two-dimensional structure that is composed of a periodic array of small scattering elements whose dimensions and periods are small when compared with the operating wavelength [2]. Due to their succinct planar structure, easy fabrication, and low cost, metasurfaces are widely used in the design of planar antennas. The main benefits of metasurface antennas are their ability to provide enhanced performance in terms of gain, radiation pattern, and bandwidth with an ultra-low profile design [3], [4]. The extraordinary properties of such antennas, which render them suitable for the application at hand, from the microwave to the terahertz band, have previously been presented [5]–[15].

In particular, researchers have focused on terahertz (THz) metasurface antennas, since the THz band has exhibited significant potential in relation to emerging applications in the fields of imaging, sensing, and astronomy, as well as defense and security [16]. This band offers many additional advantages, including an extremely high data transmission rate, wide bandwidth, high resolution, and improved spatial directivity with system compactness in wireless communication systems. Recently, a wide-gain-bandwidth metasurface antenna fed by a single open-ended, leaky-wave slit at terahertz frequencies was reported [17]. However, the higher atmospheric losses and attenuation of the THz band may restrict its usage due to its low gain. Therefore, low-profile antennas featuring high gain characteristics are highly recommended for terahertz applications.

Typically, planar antennas are coupled with lenses in order to realize high gain and wide bandwidth characteristics in the THz frequency range. Yet, lens-coupled antennas have a number of limitations, including their bulky size and low radiation efficiency [18]. Fabry-Perot antennas are designed to obtain a high gain, although such antennas face the design challenges associated with a low 3-dB gain bandwidth, especially when coupled with high-permittivity substrates [19]–[21]. THz antennas fed by slot waveguides also present high gain properties due to their low feeding losses. However, the manufacturing cost of such antennas is generally very high, since they usually consist of a complicated three-dimensional structure built with metallic walls [22], [23].

In this paper, we present the design of planar, low-profile, multiple-feed metasurface antennas with different numbers of patch cells and different substrate thicknesses in the THz frequency band in order to obtain high gain characteristics.

The remainder of this paper is organized as follows. Section II describes the geometry of the proposed antennas. Section III characterizes the detailed simulation setup as well as the conditions adopted during the numerical analysis of the antennas. Section IV presents

the antenna characteristics for different numbers of patch cells at different substrate thickness values. Finally, our conclusions are drawn in Section V.

II. SIMULATION SETUP

The majority of antenna analysis techniques can be categorized into two methods, namely a full-wave analysis method and an approximation method based on simplifying assumptions. The term "full-wave" generally refers to electromagnetic solutions that include all the applicable wave mechanisms. Such solutions allow for the implications of the boundary conditions to an accuracy limit, while the approximation methods do not enforce boundary conditions and thus do not consider surface wave effects, mutual coupling, or perhaps even radiation. Different analysis techniques and their respective limitations in terms of analyzing metasurfaces have previously been presented [24]. For high-frequency electromagnetic applications, full-wave time-domain simulation methods are highly desirable, especially when broadband results are required [25].

In our simulations, the full three-dimensional structures of the antennas were modeled, while the characteristics were investigated using the finite-integration time-domain commercial simulator CST Microwave Studio [26]. The antennas were excited by means of a discrete port located at the gap in the short dipole, which results in a default Gaussian-shaped excitation signal being passed into the gap in the slit line at its center. This setup guarantees the stability of the simulation regardless of the simulation time. A transient time-domain solver with a hexahedral mesh type was selected, while the accuracy level was set at -40 dB. This solver allows the complete characterization of the performance of antennas at multiple frequencies during one simulation run. The simulation time is inversely proportional to the size of the smallest mesh cell, which needs to be sufficiently fine to capture all the detail of the unit cell of the metasurface. In the simulation setup, the maximum mesh size was set at approximately 2.5 μm, which is one-twentieth of a free space wavelength at 0.3 THz. CST simulates each port independently, which means that the simulation time for each antenna is linearly proportional to its number of ports. Far-field monitors were set up for frequencies ranging from 0.3 THz to 0.42 THz. Moreover, open boundaries with some added space ($\lambda_o/4$) were used for the accurate calculation of the far-field results. The number of mesh cells in the computational domain for the antenna at $H =$ 40 μm with a patch number of 5×5 was approximately 1.53×10^6, occupying 1.0 GB of memory. It took about 50 minutes when using 20 threads of parallelization in the Xeon E5-2660-V2 server with a clock speed of 2.2 GHz.
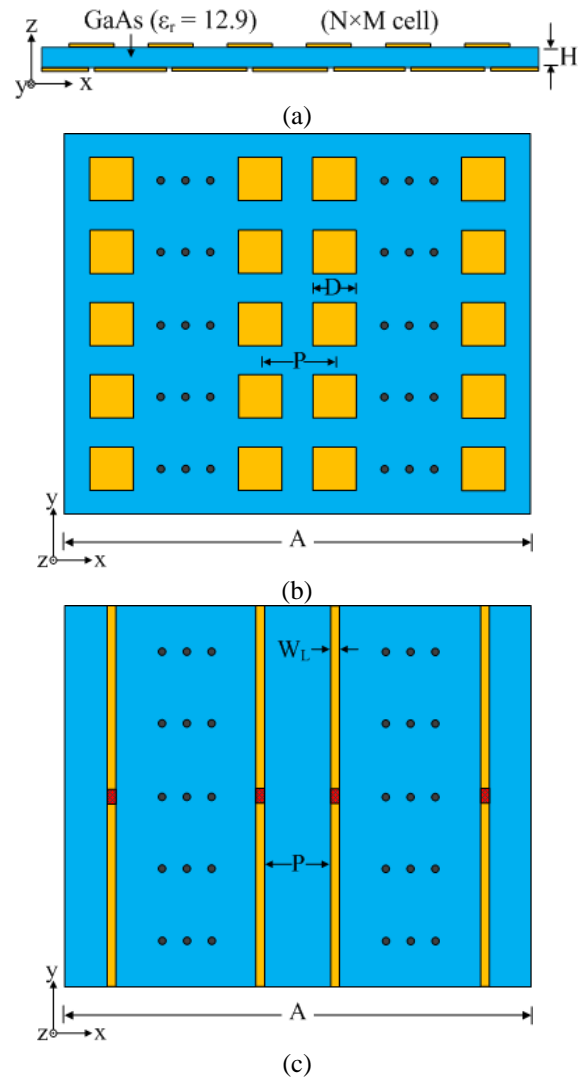

Fig. 1. Antenna geometry: (a) side view, (b) front view of top surface, and (c) front view of bottom surface.

Table 1: Common antenna design parameters

Parameter	Dimension (μm)
A	$5 \times P + D/2$
W_L	15
L_D	10
g	10

Table 2: Design parameters for different substrate thickness (H) values

| Substrate thickness (H)	Periodicity (P)	Patch Length (D)
80 μm	330 μm	195 μm
40 μm	340 μm	200 μm
20 μm	360 μm	210 μm

III. ANTENNA GEOMETRY

The geometry of the proposed metasurface antenna with a multiple-feeding structure is shown in Fig. 1. The antenna was patterned on both sides of a GaAs substrate with a dielectric constant of $\varepsilon_r = 12.9$ and a loss tangent of $tan\delta = 0.006$. The metasurface, which comprised an array of periodic $M \times N$ symmetrical metallic square patches, was patterned on the upper side of the substrate. The number of patches along the vertical axis (y-axis) was designated as M, while N represents the patches along the horizontal axis (x-axis). The periodicity and patch length of the square patch array were defined as P and D, respectively. The feeding structure, which comprised an array of open-ended, leaky-wave slits with a width of W_L, was etched on the lower side of the substrate. The number of feeding slits was equal to M, while the distance between the slits was P, which is equal to the periodicity (P) of the patch array. The chosen structure ensures the excitation of every patch column of the metasurface. The thickness and conductivity of the metal layer used in the ground plane and the patches were 0.35 μm and 1.6×10^7 S/m, respectively. The overall dimensions of the antenna were $A \times A \times H$ μm³. Each feeding slit was fed by a short dipole at its center, which had a gap and a width of g and L_D, respectively. A discrete port was placed at the center of the feed gap of each slit in order to excite the antenna. The antenna was optimized at each substrate thickness value ($H = 20$ μm, $H = 40$ μm, and $H = 80$ μm) for different numbers of patch cells ($M \times N$) by changing only the periodicity and the patch size. The design parameters of the antennas that result in the optimum broadside gain and 3-dB gain bandwidth are summarized in Tables 1 and 2. The designed antenna can be realized by feeding it with a femtosecond laser pump. The laser pulses could be simultaneously focused on the short dipole gap of each slit of the antenna so as to achieve the advantages of a low profile, high gain, and wide bandwidth characteristics.

IV. ANTENNA CHARACTERISTICS

Figure 2 shows the performance of the multiple-feed metasurface antennas in terms of the boresight gain for different numbers of patch cells and various substrate thickness values. We fixed the number of patch cells along the vertical axis because the leaky-wave slit can effectively excite up to five patch cells. Increasing the number of patch cells in the vertical direction had no significant effect on the enhancement of antenna gain [27]. Thus, we fixed the number of patch cells in the vertical direction and only increased the number of patch cells in the horizontal direction. When the number of patch cells was increased from 5×3 to 5×6 to 5×12 for different substrate thickness values ($H = 20$ μm,

$H = 40$ μm, and $H = 80$ μm), the antenna gain increased in a linear fashion. The gain increased in 3-dB increments regardless of the substrate thickness when the total number of patches was increased twice. The gain observed for 5×3 patch cells at $H = 20$ μm was 12.5 dBi, which increased to 15.5 dBi and 18.5 dBi when the number of patch cells was increased to 5×6 and 5×12, respectively. Similarly, at substrate thicknesses of $H = 40$ μm and $H = 80$ μm, the antenna gain increased from 13.5 to 19.5 dBi in a 3-dB increment when the number of patch cells increased from 5×3 to 5×6 and 5×12, respectively. These results showed that a peak gain occurs for each substrate thickness value, while the antenna gain increases with an increasing number of patch cells. Moreover, the central frequency shifted downwards for thicker substrates due to the increase in the effective dielectric constant. It was approximately 0.385 THz at $H = 20$ μm, although it shifted to 0.375 and 0.33 THz for $H = 40$ μm and $H = 80$ μm, respectively. It was interesting to observe that the 3-dB gain bandwidth and central frequency changed significantly with varying substrate thicknesses, whereas the patch number had a negligible influence on both. The 3-dB gain bandwidth was low, being approximately 8% and 10% for $H = 20$ μm and $H = 80$ μm, respectively, although it was wide, being almost 17.3% for $H = 40$ μm regardless of the patch number. In fact, the antennas with thick substrates faced the design challenges associated with a low 3-dB gain bandwidth at terahertz frequencies due to the substrate resonance. This problem can be solved by reducing the substrate thickness to $\lambda_o/20$, where λ_o, is the free-space wavelength [28]. A substrate thickness of 40 μm is approximately $\lambda_o/20$ with respect to its central operating frequency. Hence, it exhibited the wide gain bandwidth.

Figure 3 presents the radiation efficiency of the multiple-feed metasurface antennas with different numbers of patch cells at various substrate thickness values. The radiation efficiency increased with an increasing substrate thickness, although it was not affected by different patch numbers (5×3, 5×6, and 5×12), especially within the 3-dB gain bandwidth. The radiation efficiency calculated for $H = 20$ μm was 57%, which increased to 73% and 85% for $H = 40$ μm and $H = 80$ μm, respectively. It was observed that the number of patch cells only influenced the gain enhancement, without significantly changing the other antenna characteristics, whereas the substrate thickness determined both the 3-dB gain bandwidth and the radiation efficiency. This therefore provides a simple method for determining the specific antenna characteristics in terms of both gain and bandwidth by choosing a specific combination of patch number ($M \times N$) and substrate thickness.
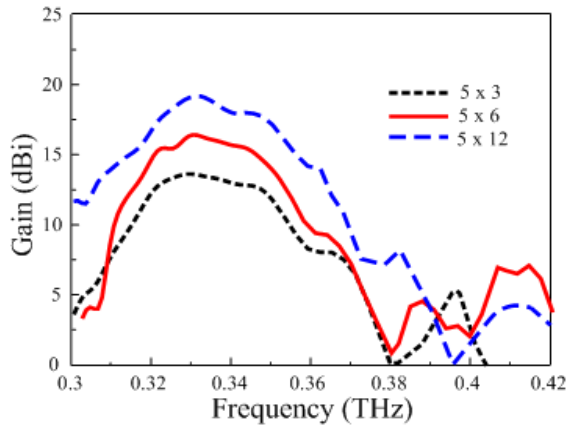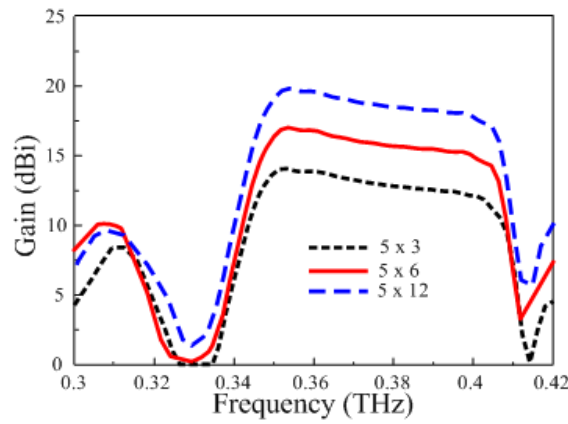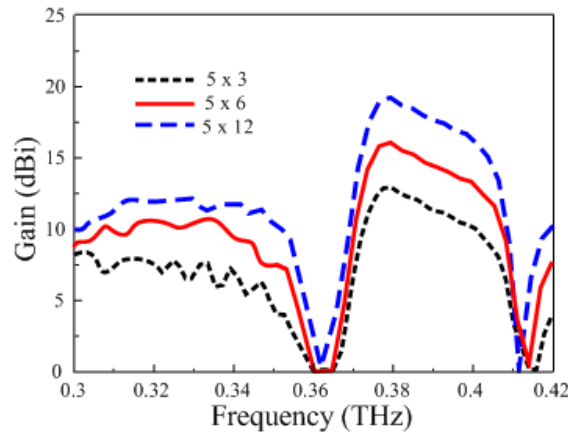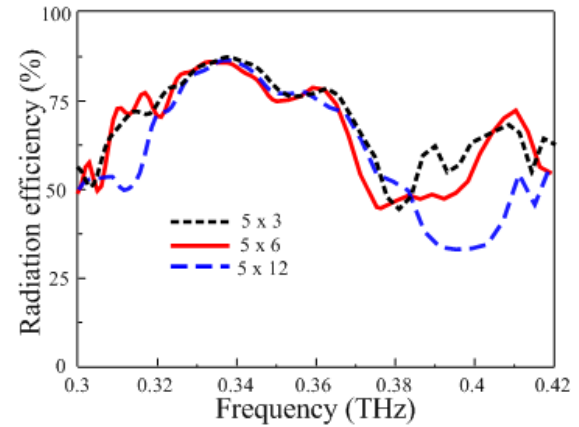
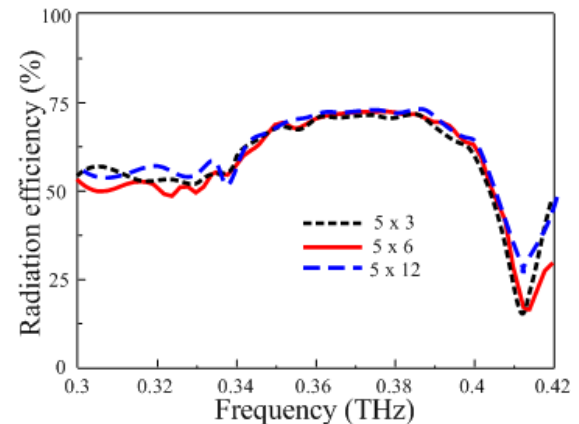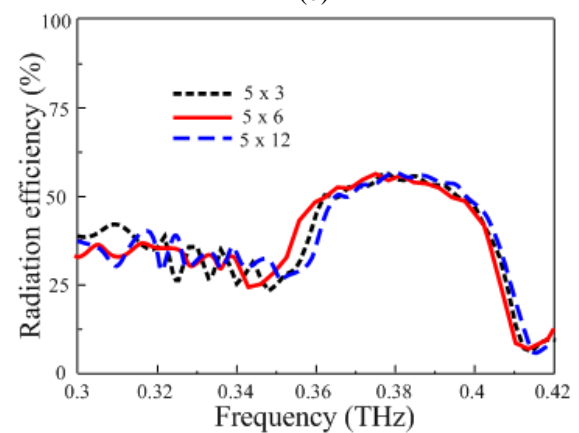Fig. 2. Antenna gain with different numbers of patch cells and different substrate thicknesses: (a) $H = 80$ µm, (b) $H = 40$ µm, and (c) $H = 20$ µm.

Fig. 3. Antenna radiation efficiency with different numbers of patch cells and different substrate thicknesses: (a) $H = 80$ µm, (b) $H = 40$ µm, and (c) $H = 20$ µm.
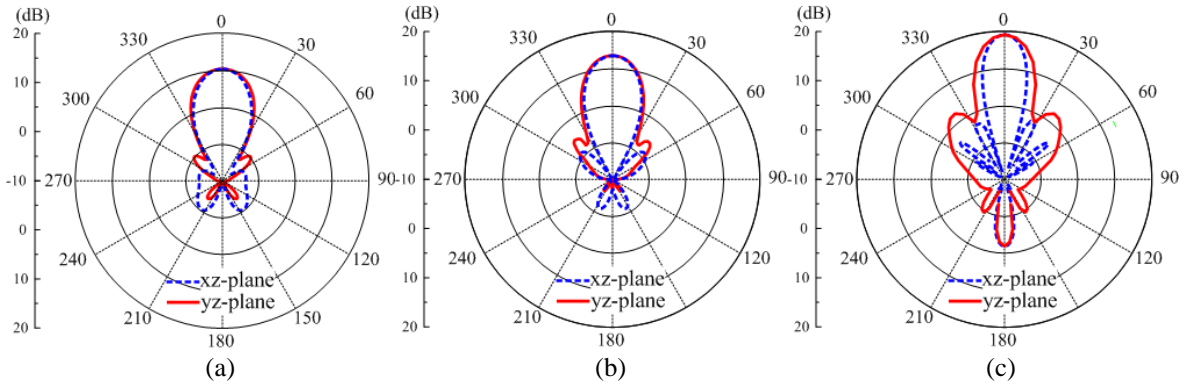
Fig. 4. Antenna radiation patterns for different numbers of patch cells at $H = 80$ µm: (a) 5×3, (b) 5×6, and (c) 5×12.
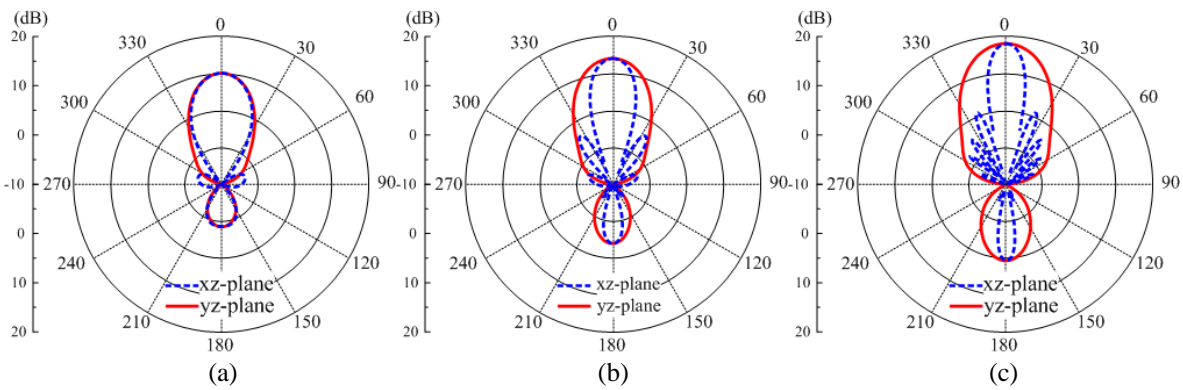

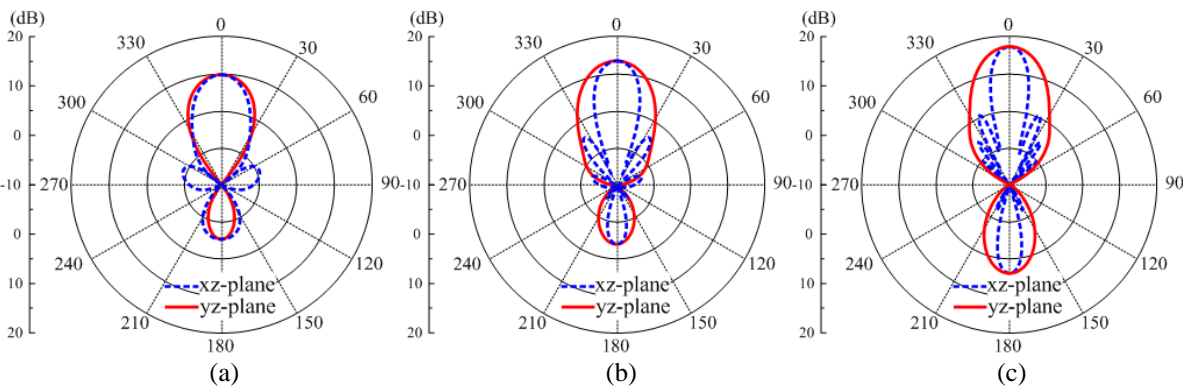Fig. 5. Antenna radiation patterns for different numbers of patch cells at $H = 40$ µm: (a) 5×3, (b) 5×6, and (c) 5×12.

Fig. 6. Antenna radiation patterns for different numbers of patch cells at $H = 20$ µm: (a) 5×3, (b) 5×6, and (c) 5×12.

The radiation patterns of the metasurface antennas with different substrate thicknesses and different patch numbers were plotted at their central frequencies as shown in Figs. 4–6. All the antennas exhibited directive radiation patterns with low sidelobe and backlobe levels in both the *xz*- and *yz*-planes. Generally, the *yz*-plane showed clean profile patterns with lower sidelobe levels when compared to the *xz*-plane. Furthermore, the number of sidelobe levels in the *xz*-plane increased with an increasing number of patch cells. The antennas yielded low back radiation throughout the entire gain bandwidth due to the successful implementation of the metasurface, even though the leaky-wave slit is open to free space. However, the gain value associated with both

back radiations increased with an increase in the number of patch cells. Interestingly, the back radiation decreased when the substrate thickness increased.

V. CONCLUSION

The design of multiple-feed metasurface antennas with different numbers of patch cells and different substrate thicknesses, as well as the associated radiation characteristics, were studied over the THz frequency band. The antennas were composed of a patch array and multiple feeding structures, both of which were patterned on a high-permittivity, electrically thin GaAs substrate. Regardless of the substrate thickness, the antenna gain increased linearly in increments of 3 dB when the number of patches was increased twice. The radiation efficiency and 3-dB gain bandwidth were mainly determined by the substrate thickness. The 3-dB gain bandwidth was 7%, 17.3%, and 10% for the substrate thicknesses of $H = 20$ µm, $H = 40$ µm, and $H = 80$ µm, respectively. The radiation efficiency increased with increasing substrate thickness. The efficiency was calculated as 57% at $H = 20$ µm, and it increased to 73% for $H = 40$ µm and 85% for $H = 80$ µm. The different combinations of patch numbers and substrate thicknesses provide freedom in terms of choosing the desired gain values and 3-dB gain bandwidth for various antenna applications, which increases their value for THz applications. Furthermore, these antennas offer a number of other promising features, including a low profile, mechanical robustness, suitability for low-cost mass production, and easy integration into circuit boards.

REFERENCES

[1] N. Yu and F. Capasso, "Flat optics with designer metasurfaces," *Nat. Mater.*, vol. 13, no. 2, pp. 139-150, 2014.

[2] J. P. Turpin, J. A. Bossard, K. L. Morgan, D. H. Werner, and P. L. Werner, "Reconfigurable and tunable metamaterials: A review of the theory and applications," *Int. J. Antennas Propag.*, vol. 2014, 429837, pp. 1-18, 2014.

[3] Y. Dong and T. Itoh, "Metamaterial-based antennas," *Proc. IEEE*, vol. 100, no. 7, pp. 2271-2285, 2012.

[4] C. L. Holloway, E. F. Kuester, J. A. Gordon, J. O'Hara, J. Booth, and D. R. Smith, "An overview of the theory and applications of metasurfaces: The two-dimensional equivalents of metamaterials," *IEEE Antennas Propag. Mag.*, vol. 54, no. 2, pp. 10-35, 2012.

[5] M. Koutsoupidou, I. S. Karanasiou, and N. Uzunoglu, "Rectangular patch antenna on split-ring resonators substrate for THz brain imaging: Modeling and testing," *IEEE Int. Conf. on Bio-informatics and Bioengineering*, Chania, Greece, pp. 1-4, Nov. 2013.

[6] M. E. Badawe, T. S. Almoneef, and O. M. Ramahi, "A true metasurface antenna," *Sci. Rep.*, vol. 6, 19268, pp. 1-8, 2016.

[7] H. Zhou, J. Dong, S. Yan, Y. Zhou, and X. Zhang, "Generation of terahertz vortices using metasurface with circular slits," *IEEE Photon. J.*, vol. 6, no. 6, 5900107, pp. 1-7, 2014.

[8] Q. Zhang, L. Si, Y. Huang, X. Lv, and W. Zhu "Low-index-metamaterial for gain enhancement of planar terahertz antenna," *AIP Adv.*, vol. 4, no. 3, 037103, pp. 1-7, 2014.

[9] Y. Huang, L. Yang, J. Li, Y. Wang, and G. Wen, "Polarization conversing of metasurface for the application of wide band low-profile circular polarization slot antenna," *Appl. Phy. Lett.*, vol. 109, 054101, pp. 1-5, 2016.

[10] N. Nasimuddin, Z. N. Chen, and X. Qing, "Bandwidth enhancement of a single-feed circularly polarized antenna using a metasurface: Metamaterial-based wideband CP rectangular microstrip antenna," *IEEE Antennas Propag. Mag.*, vol. 58, no. 2, pp. 39-46, 2016.

[11] X. Gao, X. Han, W. P. Cao, H. F. Ma, H. O. Li, and T. J. Cui, "Ultrawideband and high-efficiency linear polarization converter based on double v-shaped metasurface," *IEEE Trans. Antennas Propag.*, vol. 63, no. 8, pp. 3522-3530, 2015.

[12] A. Mahmood, G. O. Yetkin, and C. Sabah, "Wideband negative permittivity and double negative fishnet-mushroom-like metamaterial in x-band waveguide," *Int. J. Antennas Propag.*, vol. 2017, 2439518, pp. 1-7, 2017.

[13] S. I. Rosaline and S. Raghavan, "Metamaterial inspired square ring monopole antenna for WLAN applications," *ACES Express J.*, vol. 1, no. 1, pp. 32-35, 2016.

[14] A. Shater and D. Zarifi, "Radar cross section reduction of microstrip antenna using dual-band metamaterial absorber," *ACES J.*, vol. 32, no. 2, pp. 135-140, 2017.

[15] P. Rocca and A. F. Morabito, "Optimal synthesis of reconfigurable planar arrays with simplified architectures for monopulse radar applications," *IEEE Trans. Antennas Propag.*, vol. 63, no. 3, pp. 1048-1058, 2015.

[16] P. H. Siegel, "Terahertz technology," *IEEE Trans. Microw. Theory Tech.*, vol. 50, no. 3, pp. 910-928, 2002.

[17] N. Hussain and I. Park, "Terahertz planar wide-gain-bandwidth metasurface antenna," *Int. Workshop on Metamaterials-by-Design*, Riva del Garda, Italy, pp. 1-2, Dec. 2016.

[18] N. Hussain, T. K. Nguyen, H. Han, and I. Park, "Minimum lens size supporting the leaky-wave nature of slit dipole antenna at terahertz frequency," *Int. J. Antennas Propag.*, vol. 2016, 5826957, pp. 1-8, 2016.

[19] N. Hussain, K. E. Kam, and I. Park, "Performance of a planar leaky-wave slit antenna for different values of substrate thickness," *J. Electromagn. Eng. Sci.*, vol. 17, no. 4, pp. 202-207, Oct. 2017.

[20] T. K. Nguyen, B. Q. Ta, and I. Park, "Design of a planar, high-gain, substrate-integrated Fabry-Perot cavity antenna at terahertz frequency," *Curr. Appl. Phys.*, vol. 15, no. 9, pp. 1047-1053, 2015.

[21] N. Hussain, T. K. Nguyen, and I. Park, "Performance comparison of a planar substrate-integrated Fabry-Perot cavity antenna with different unit cells at terahertz frequency," in *IEEE European Conf. on Antennas and Propagation*, Davos, Switzerland, pp. 1-4, Apr. 2016.

[22] K. M. Luk, S. F. Zhou, Y. J. Li, F. Wu, K. B. Ng, C. H. Chan, and S. W. Pang, "A microfabricated low-profile wideband antenna array for terahertz communications," *Sci. Rep.*, vol. 7, 1268, pp. 1-11, 2017.

[23] C. Gu, S. Gao, and B. Sanz-Izquierdo, "Low-cost wideband low-THz antennas for wireless comm-unications and sensing," in *UK-Europe-China Workshop on Millimetre Waves and Terahertz Technologies*, Liverpool, UK, pp. 1-4, Sep. 2017.

[24] F. Costa, A. Monorchio, and G. Manara, "An overview of equivalent circuit modeling techniques of frequency selective surfaces and metasurfaces," *ACES J.*, vol. 29, no. 12, pp. 960-976, Dec. 2014.

[25] A. Taflove and S. C. Hagness, *Computational Electromagnetics: The Finite-Difference Time-Domain (FDTD) Method*. Artech House, 3rd ed., 2005.

[26] CST Microwave Studio, https://www.cst.com/

[27] N. Hussain and I. Park, "Design of a wide-gain-bandwidth metasurface antenna at terahertz frequency," *AIP Adv.*, vol. 7, no. 5, 055313, pp. 1-8, 2017.

[28] B. A. Munk, *Frequency Selective Surfaces: Theory and Design*. Wiley, New York, 2000.
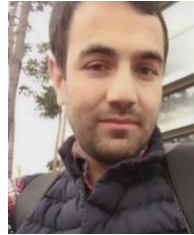
Niamat Hussain received his B.S. degree in Electronics Engineering from Dawood University of Engin-eering and Technology, Karachi, Pakistan, in 2014. He is currently studying for his M.S. degree at the Department of Electrical and Computer Engineering at Ajou University, Suwon, Republic of Korea. His research is mainly focused on lens-coupled antennas, metasurface antennas, and terahertz antennas.

Ikmo Park received his B.S. degree in Electrical Engineering from the State University of New York at Stony Brook and his M.S. and Ph.D. degrees in Electrical Engineering from the University of Illinois at Urbana-Champaign. He joined the Department of Electrical and Computer Engineering at Ajou University in 1996. Prior to joining Ajou University, he was with the Device and Materials Laboratory, LG Corporate Institute of Technology, Seoul, Republic of Korea, where he was engaged in research and development of various antennas for personal communication systems, wireless local area networks, and direct broadcasting systems. He has authored and co-authored over 300 technical journal and conference papers. He also holds over 30 patents. His current research interests include the design and analysis of microwave, millimeter-wave, terahertz wave, and nano-structured antennas.